Quenched monopoles in lattice gauge theory

Daniel R. Stump
Department of Physics and Astronomy, Michigan State University, East Lansing, Michigan 48824
(Received 20 July 1988)

Monopole configurations are created by a relaxation method, for Abelian and non-Abelian lattice gauge theories. The difference between the density of quenched monopoles from the high- and low-energy phases, at the phase transition of the O(3) and O(2) gauge theories, is discussed.

I. INTRODUCTION

The role of magnetic-monopole configurations in lattice gauge theory has been an interesting question since the observation[1] that monopoles would create the kind of disorder in the gauge field needed for linear quark confinement. There have been speculations on the nature of monopoles in three- and four-dimensional models,[2,3] and Monte Carlo studies of monopoles.[4] Recent research,[5] specifically on monopoles in non-Abelian gauge theories, has furthered the interest in this topic.

The purpose of this paper is to describe a study of magnetic-monopole configurations created by relaxation calculations for Abelian and non-Abelian gauge theories in three and four dimensions. This is particularly interesting in models with a phase transition, such as the O(2) and O(3) gauge theories in four dimensions. It will be shown that the density of monopoles after relaxation is very different for equilibrium states just above and below the transition. The relaxation process is like a quenching process, in which the gauge field is suddenly cooled to zero temperature. Monopoles are topologically stable defects, which are frozen in the gauge field by the quenching. Thus, the density of monopoles after relaxation is a measure of the disorder due to topological defects in the state from which the relaxation begins.

The outline of the paper is as follows. Section II defines the method of relaxation calculation used, and describes the results of calculations in a three-dimensional lattice. Section III describes results in a four-dimensional lattice, for relaxation from states near the phase transition. Section IV is a discussion of the implications of the study.

II. RELAXATION CALCULATIONS IN THREE DIMENSIONS

Let $U(l)$ denote the link variable of a lattice gauge theory. For an SU(2) gauge theory, $U(l)$ has the form

$$U(l)=U_4(l)+i\boldsymbol{\sigma}\cdot\mathbf{U}(l)\ , \tag{1}$$

where

$$U_4^2(l)+\mathbf{U}^2(l)=1\ . \tag{2}$$

For an O(2) gauge theory, which is equivalent to a U(1) gauge theory, $U(l)$ has the form

$$U(l)=U_4(l)+i\sigma_3 U_3(l)\ , \tag{3}$$

where

$$U_4^2(l)+U_3^2(l)=1\ . \tag{4}$$

The plaquette variable $U(p)$ has a similar representation. The partition function of the lattice gauge theory is

$$Z=\int \exp(-\beta E)\prod_l d\mu[U(l)]\ , \tag{5}$$

where E denotes the action of the theory, and $d\mu[U]$ the appropriate group measure. The fundamental action of the SU(2) gauge theory is[6]

$$E=\sum_p [1-U_4(p)]\ ; \tag{6}$$

the adjoint action of the SU(2) gauge theory, which I shall refer to as the O(3) action, is[7,8]

$$E=\tfrac{4}{3}\sum_p [1-U_4^2(p)]\ . \tag{7}$$

The action of the O(2) gauge theory can be defined to be[9] either

$$E=\sum_p [1-U_4(p)] \tag{8}$$

or

$$E=2\sum_p [1-U_4^2(p)]\ , \tag{9}$$

where $U(l)$ is restricted to the form (3); that the two actions are equivalent is proven in the Appendix. The factors in Eqs. (6)–(9) are such that the average action per plaquette $\bar{E}/P$ is 1 at $\beta=0$, i.e., for a random field configuration.

The relaxation calculation produces a solution of the lattice field equation

$$\frac{\partial E}{\partial U_k(l)}=0 \tag{10}$$

for all l, and for $k=1$–4 for the SU(2) and O(3) gauge theories, or $k=3$ to 4 for the O(2) gauge theory. Equation (10) may be thought of as an equation for $U(l)$, given $U(l')$ on all other links l'. The actions (7) and (9) are quadratic functions of $U_k(l)$, of the form

$$E=-\sum_{k,k'} U_k M_{k,k'} U_{k'}+R\ , \tag{11}$$

where U_k stands for $U_k(l)$, $M_{k,k'}$ depends only on the field at links that share a plaquette with l, and R is independent of $U(l)$. Then Eq. (10) is an eigenvalue equation

$$\sum_{k'} M_{k,k'} U_{k'} = \lambda U_k \ . \tag{12}$$

The actions (6) and (8) are linear functions of $U_k(l)$, of the form

$$E = \sum_k U_k N_k + R \ , \tag{13}$$

where again N_k depends on the field at links that share a plaquette with l. In this case, the solution of Eq. (10), as an equation for $U_k(l)$, is

$$U_k = -N_k / |N| \ , \tag{14}$$

where $|N|$ is the magnitude of N_k.

The idea of the relaxation calculation is simple.[10,11] Starting from the configuration of interest, Eq. (10) is solved successively for each link, keeping the other links fixed at their current values. After a sufficient number of such relaxation sweeps, the configuration converges to a solution of the lattice field equation. In particular, Eq. (14) minimizes E with respect to $U(l)$; then, if the relaxation converges, it converges to a local minimum of E. Similarly, if in Eq. (12) the relaxed value of U(l) is the eigenvector of $M_{k,k'}$ with largest eigenvalue λ, then the relaxation again converges to a local minimum of E. For a linear field equation, without sources, the relaxation procedure would converge simply to zero field. However, the field equation of lattice gauge theory is nonlinear. Therefore, there are nontrivial solutions of the field equation even without external sources; the field acts as its own source.

An example of a nontrivial field configuration is a monopole solution, for the three-dimensional gauge theory with action (7) or (9). A monopole-antimonopole ($M\overline{M}$) pair is produced by a line of plaquettes with $U_4(p) \approx -1$. This solenoid, one plaquette wide, is the lattice approximation of a Dirac string. At the end points there is a source or sink of magnetic field, where the magnetic field refers to the plaquette field. The solenoid is unobservable, in the sense that plaquettes with $U_4(p) = -1$ have zero action. The $M\overline{M}$ configuration is a stable, or at least metastable, solution of the O(2) and O(3) gauge theories in three dimensions.[10,11] There is an action barrier against unwinding the gauge field around the solenoid, because the Dirac string has zero action.

A problem in studying monopoles in the gauge field is to identify them. It is possible to define a topological winding number to identify monopoles.[4] However, in this paper I shall identify monopoles by looking at two gauge-invariant quantities related to the action. First, I define a plaquette value $P(p)$, which is proportional to the action of the plaquette p, by

$$P(p) = 1 - U_4^2(p) \ ; \tag{15}$$

the range of $P(p)$ is from 0 to 1. Second, I define a cube value for the elementary cube at site x by

$$C(x) = \sum_{6p} P(p) \ , \tag{16}$$

where the sum is over the six plaquettes that are the faces of the cube; the range of $C(x)$ is from 0 to 6. It will be shown that monopoles in a relaxed field configuration are easily identified using these quantities, especially C.

Figure 1 shows an $M\overline{M}$ pair in the O(3) lattice gauge theory in three dimensions, in a 10^3 lattice. This configuration was constructed[10,11] by relaxing from an initial configuration with a Dirac string of length four lattice spacings. That is, initially the links around the solenoid have $U(l) = (1 \pm i\sigma_3)/\sqrt{2}$, with the signs chosen such that $U(p) = -1$ for the plaquettes perpendicular to the solenoid. During the relaxation, the magnetic flux spreads out from the ends of the string, but the topological singularities initially present remain after relaxation. Actually the result is just an O(2) $M\overline{M}$ pair embedded in the O(3) gauge field.

The two quantities P and C are exhibited in Fig. 1 in different ways. First, the gradient of the plaquette value P is drawn wherever its magnitude is greater than 0.04. The gradient is a vector field defined at the centers of the elementary cubes of the lattice; the ith component of grad(P) at the cube at site x is $P(x + e_i, jk) - P(x, jk)$ where (ijk) is a cyclic permutation of (123). Second, the cube value C is exhibited by drawing a small cube wherever $C \geq 1.4$. The figure projects out the $M\overline{M}$ pair very clearly, because large C and large grad(P) only occur at a monopole site. The Dirac string connecting the pair is invisible. The gradient grad(P) decreases rapidly with distance from the monopole; only the six cubes nearest an isolated monopole have $|\text{grad}(P)| \geq 0.04$. In the O(2) gauge theory it is possible to exhibit the monopoles more directly by plotting the magnetic field $B(p)$ throughout the lattice.[10,11] The field $B(p)$ decreases more slowly than grad(P), but rapidly enough to identify monopoles isolated by several lattice spacings. However, for the

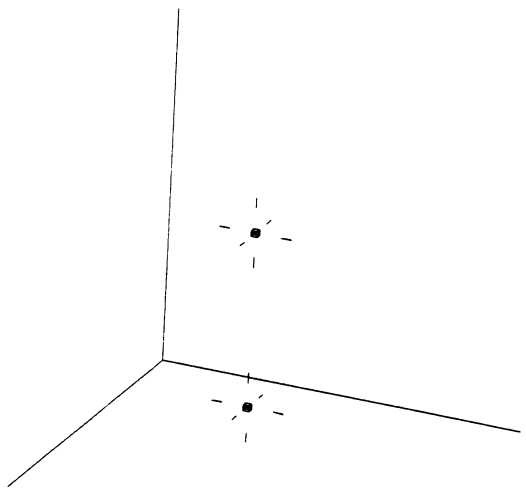

FIG. 1. Monopole-antimonopole configuration in a 10^3 lattice. The vector grad(P) is drawn if its magnitude is greater than 0.04, and a small cube is drawn at site x if $C(x) > 1.4$.

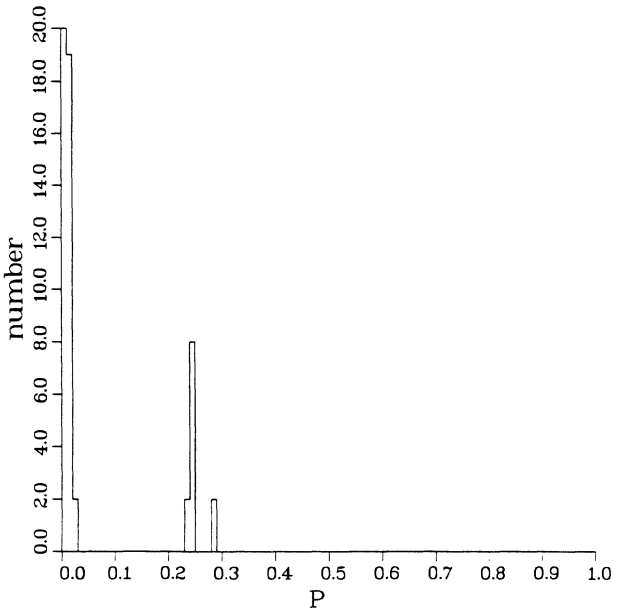

FIG. 2. Histogram of P for the configuration in Fig. 1.

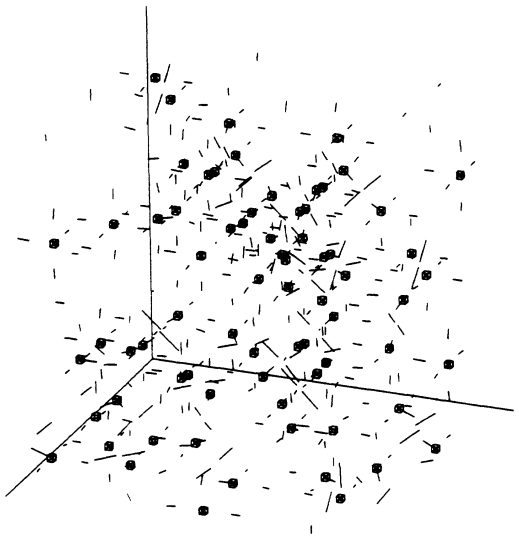

FIG. 4. Quenched monopoles in the O(3) gauge theory in a 10^3 lattice. The configuration was created by a relaxation calculation starting from an equilibrium configuration at $\beta=0$. The quantities grad(P) and C are drawn as in Fig. 1.

O(3) gauge theory the magnetic field $B_a(p)$ has three components in the gauge group space, and the individual components are not gauge invariant, so this is not a convenient way to exhibit O(3) monopoles.

Figure 2 shows a histogram of plaquette value P for the configuration in Fig. 1; the width of the P bins is 0.01. Figure 3 shows a histogram of the cube values C of elementary cubes for the configuration in Fig. 1; the width of the C bins is 0.05. The two elementary cubes with $C \approx 1.5$ are the locations of the monopole and antimonopole. The value of C for these cubes can be explained, as follows. For an O(2) monopole in three dimensions, the total flux is equal to 2π, shared among the six plaquettes that surround the monopole. If the energy is shared equally, then $B(p)=\pi/3$ for the six plaquettes; then the plaquette value $P(p)$ is

$$1-\cos^2\tfrac{1}{2}B(p)=\tfrac{1}{4}\ .$$

Thus, the cube value C at the monopole site is $\frac{6}{4}$. More precisely, Fig. 2 shows that the 12 plaquettes nearest the monopole or antimonopole have P between 0.23 and 0.27; evidently the six plaquettes surrounding the monopole do not share the flux equally, due to the presence of the other member of the $M\bar{M}$ pair.

Figures 4–6 show the configuration that results from

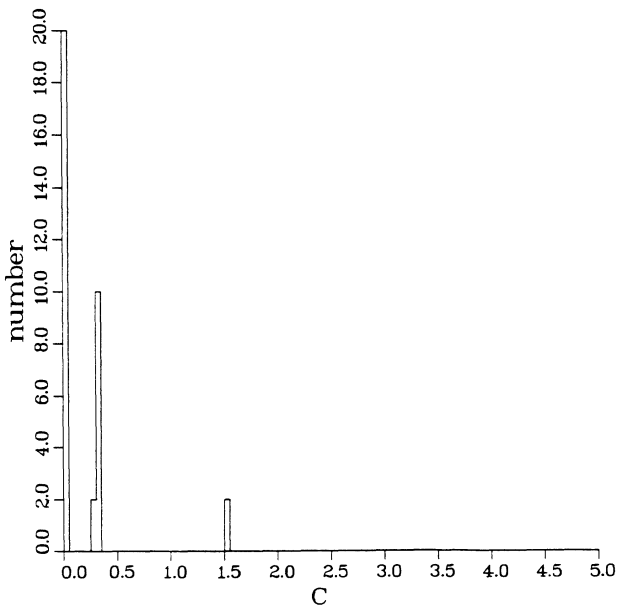

FIG. 3. Histogram of C for the configuration in Fig. 1.

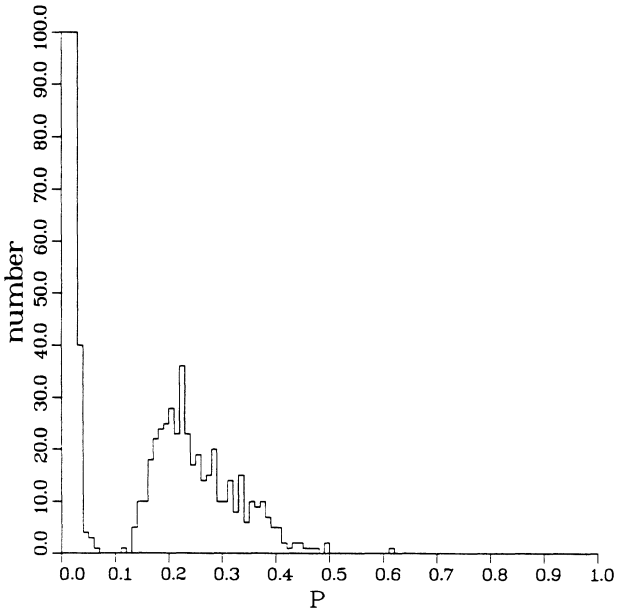

FIG. 5. Histogram of P for the configuration in Fig. 4.

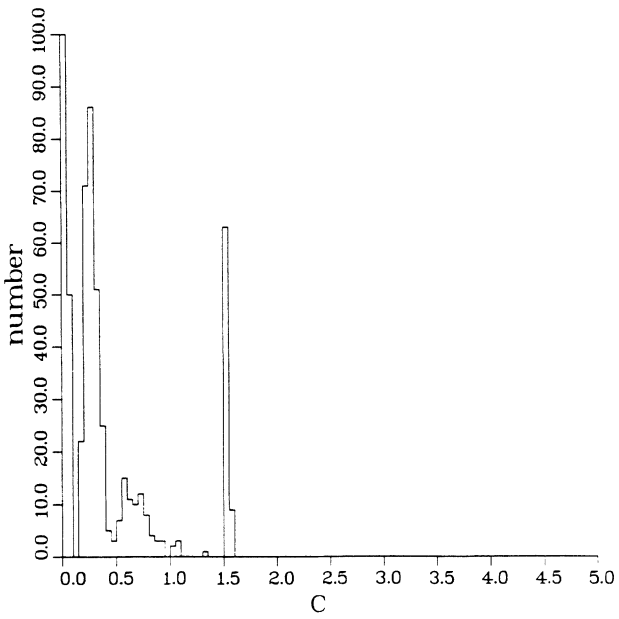

FIG. 6. Histogram of C for the configuration in Fig. 4.

relaxing a typical random configuration of the O(3) gauge field in three dimensions. The lattice size is 10^3, with periodic boundary conditions. The starting configuration was an equilibrium configuration for $\beta=0$, generated by a Monte Carlo calculation. Figure 4 shows grad(P) and C for the relaxed configuration as in Fig. 1, and Figs. 5 and 6 show histograms of P and C, respectively. The 10^3 lattice is filled with monopoles, but individual monopoles are still identifiable. The configuration in Fig. 4 looks very disordered, but in fact its action is very small; the action per plaquette $\bar{E}/P$ is 0.0567. The number of monopoles in the configuration is 72, in a 10^3 lattice, corresponding to a monopole density of 0.072; thus the mean volume occupied by a monopole is $13.9a^3$, where a is the lattice spacing. Even though the density is large, the histograms of P and C show similar profiles to those for the well-separated $M\bar{M}$ pair. Therefore, it is not necessary to look at a picture such as Fig. 4 to identify monopoles in the field; it is sufficient to examine the histograms of P and C for the configuration. In particular, each monopole is associated with a cube with $C\approx 1.5$.

The relaxed configurations shown in Figs. 1–6 are for an O(3) gauge field. Similar configurations result for an O(2) gauge field in three dimensions. Histograms of P and C for relaxed O(2) configurations are virtually the same as those for O(3) configurations. In the O(2) case one can plot the magnetic field $B(p)$, and verify that the peak in C at $C\approx 1.5$ is caused by sources and sinks of $B(p)$. It is interesting that the topological configurations of the three-dimensional O(3) and O(2) gauge theories are so similar. Apparently the monopole of the O(3) lattice field is just an embedded O(2) monopole, or a gauge transformation of it.

In the relaxation calculations, multimonopole configurations such as those in Figs. 1 and 4 seem to be absolutely stable. The convergence can be followed by observing the decrease in the action E, as the field relaxes to a local minimum of E. The convergence is rapid: the field changes very little after the first few relaxation sweeps. Apparently this creates a configuration in which the monopoles and antimonopoles are sufficiently far apart that further relaxation does not cause them to annihilate, at least not by this one-link-at-a-time relaxation process.

III. QUENCHED MONOPOLES AND FOUR-DIMENSIONAL PHASE TRANSITIONS

Both the O(3) and O(2) lattice gauge theories in four dimensions have a phase transition, which separates a disordered phase at small β from a phase at large β in which the typical field configuration is strongly correlated in spacetime. Figure 7 shows the average action per plaquette $\bar{E}/P$ as a function of β for the O(3) gauge theory, computed by Monte Carlo calculations on a 5^4 lattice. At the phase transition point, $\beta_c\approx 2.55$, there are two equilibrium phases. The equilibrium state is at the minimum of the "free-energy" function $F(E)=E-S(E)/\beta$, where $S(E)$ is the entropy at action E defined as the log of the density of states. The hysteresis loop in Fig. 7 shows that $F(E)$ has a double minimum for $\beta=\beta_c$ (Refs. 12 and 13). The latent heat of the phase transition is the difference in E between the two minima of $F(E)$ at $\beta=\beta_c$. For β near β_c, in the hysteresis region, $F(E)$ still has two local minima, so there are two metastable phases. Only when β is sufficiently far from β_c is there a single local minimum of $F(E)$, i.e., a single equilibrium phase. Figure 8 shows the average action per plaquette $\bar{E}/P$ as a function of β for the O(2) gauge theory, which has a phase transition at $\beta_c\approx 1.0$.

An interesting problem is to characterize the difference between the two equilibrium phases at $\beta=\beta_c$. In this section I describe the configurations that result from relax-

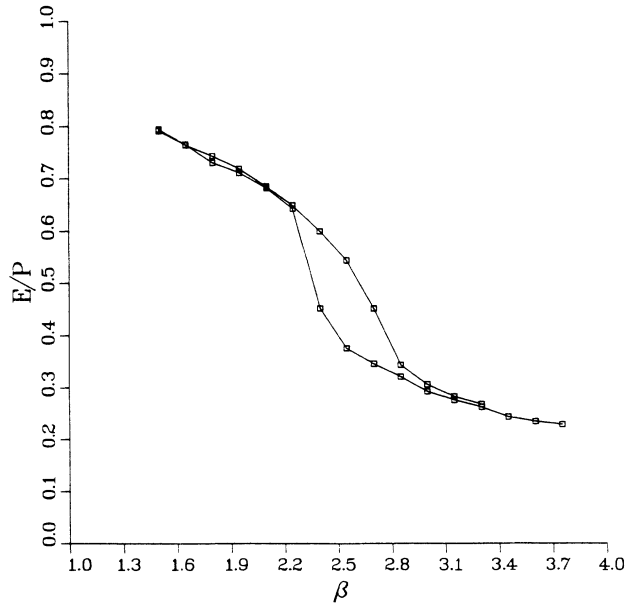

FIG. 7. Hysteresis loop at the phase transition of the O(3) gauge theory.

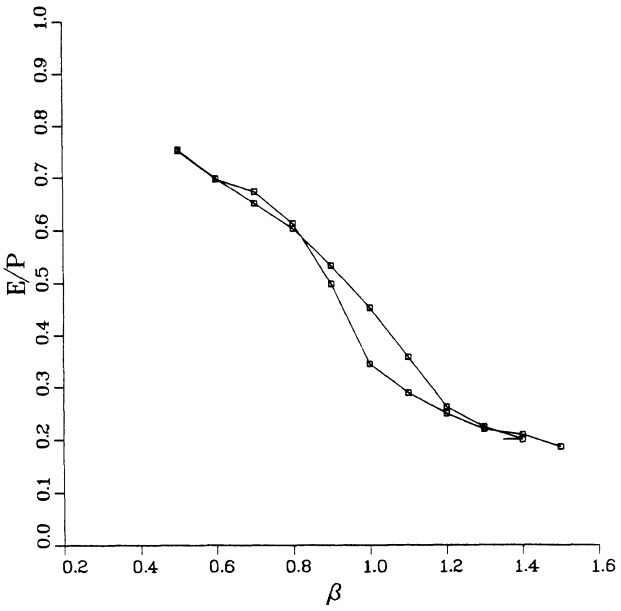

FIG. 8. Hysteresis loop at the phase transition of the O(2) gauge theory.

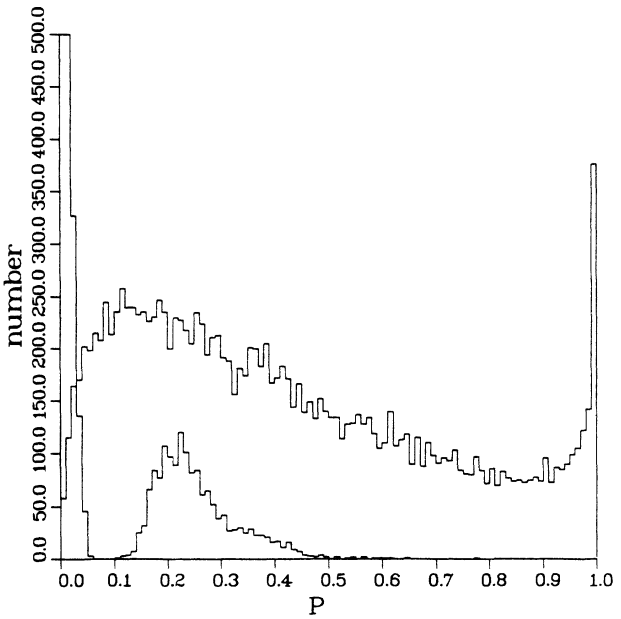

FIG. 9. Histogram of P for an equilibrium configuration of the large-E phase of the O(3) gauge theory at $\beta=2.55$ (the broad distribution) and for the quenched configuration (sharply peaked at $P=0$ and in the region $0.1 \leq P \leq 0.3$).

ing typical equilibrium configurations of these phases. The relaxation calculation is done only on the three-dimensional time slices of the four-dimensional lattice, i.e., three-dimensional subspaces at constant x_4. The calculations are for a lattice of size $10^3 \times 5$. The equilibrium configuration to be relaxed is created by a Monte Carlo calculation for $\beta=\beta_c$, in the full four-dimensional space-time. Then the relaxation calculation is done independently for each of the five time slices, each of size 10^3. That is, in relaxing the gauge field in a given time slice, the field is treated as a three-dimensional field only, consisting of spacelike links with interactions between links in the same time slice, but with no interactions with the links in other time slices, nor with any timelike links. The relaxation calculation for each time slice is the same as the three-dimensional calculation described in Sec. II. Thus, the relaxation calculation minimizes the three-dimensional *magnetic energy* of the gauge field in each time slice, but not the four-dimensional action. This procedure is intended to project out magnetic monopoles in the time slices, which originate in the four-dimensional equilibrium field.

The relaxation process can be thought of as a *quenching* process, in which the temperature $1/\beta$ is suddenly reduced to zero. The quenching eliminates high-frequency fluctuations of the field. However, topological configurations, i.e., configurations that are local minima of the energy but with a topological singularity, present in the initial configuration, will be frozen in the field after quenching. Thus, by examining the quenched configuration, I can study the presence of monopoles in the initial equilibrium state. This technique has been used to study vortices in the planar spin model,[14] and instantons in the SU(2) lattice gauge theory.[15] The result of the calculations is that the density of monopoles after quenching is almost 0 in the small-E phase, but significantly greater than 0 in the large-E phase, at $\beta=\beta_c$.

Figure 9 shows histograms of plaquette value P for two O(3) gauge-field configurations. The first configuration is an equilibrium configuration at $\beta=2.55$ in the large-E phase; the action per plaquette $\bar{E}/P$ in this initial configuration is 0.5525, consistent with the large-E phase in the hysteresis loop in Fig. 7. The second configuration is the quenched configuration that results from relaxing the first configuration; the (three-dimensional) action per plaquette in the quenched configuration is 0.0409. Figure 10 shows histograms of cube value C for these two

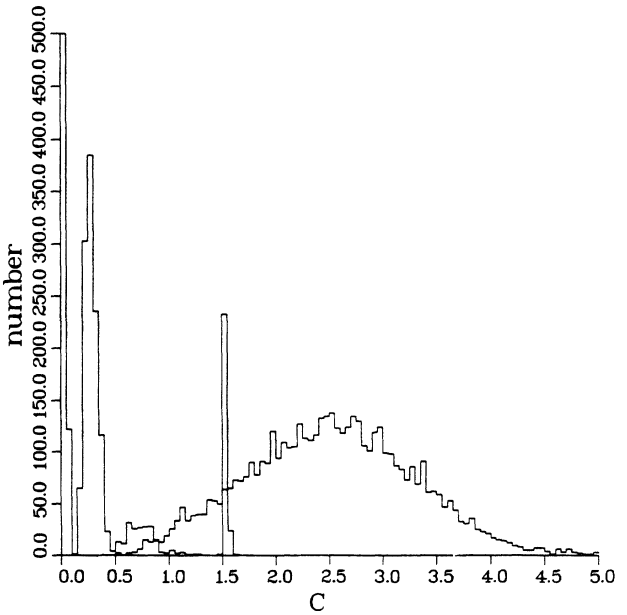

FIG. 10. Histogram of C for the same configurations as Fig. 9.

configurations. The initial configuration has broad distributions of P and C. In contrast, the quenched configuration has distributions of P and C that are the same as for a superposition of monopoles, sharply peaked at 0 but with some C near 1.5 from isolated monopoles. The number of quenched monopoles, which is just the number of elementary cubes with $C \approx 1.5$, is 259; or, since there are 5×10^3 cubes in the five time slices, the mean density of quenched monopoles is 0.052 in any three-dimensional time slice. This is to be compared to the monopole density 0.072 of the configurations shown in Fig. 4.

Figures 11 (and 12) show histograms of P (and C) for an equilibrium O(3) gauge field configuration in the small-E phase at $\beta = 2.55$, and the corresponding quenched configuration. The average action per plaquette $\bar{E}/P$ is 0.3754 in the initial configuration, consistent with the small-E phase in the hysteresis loop in Fig. 7; and $\bar{E}/P$ is 0.0023 in the quenched configuration. In this case the number of quenched monopoles is only 12, corresponding to a mean density of 0.002 in any time slice. The density of quenched monopoles is much smaller in the small-E phase than in the large-E phase.

There is a measurable difference between the equilibrium states before quenching. The histograms of P and C are visibly shifted to higher P and C in the large-E phase. However, in both cases the equilibrium-state distributions are rather broad, and extend to large P and C. What is most striking in the relaxed configurations is that there are almost no quenched monopoles from the small-E phase, even though the distribution of P and C in the equilibrium state of the small-E phase extends well beyond the values characteristic of monopoles. In other words, there is plenty of energy in the small-E equilibrium state to create monopoles; indeed the energy of the quenched state in Fig. 9 is much less than that of the small-E equilibrium state of Fig. 11. However, the energy comes from high-frequency fluctuations of the gauge field. The reason there are so few quenched monopoles from the small-E equilibrium configuration is that this state is not topologically disordered.

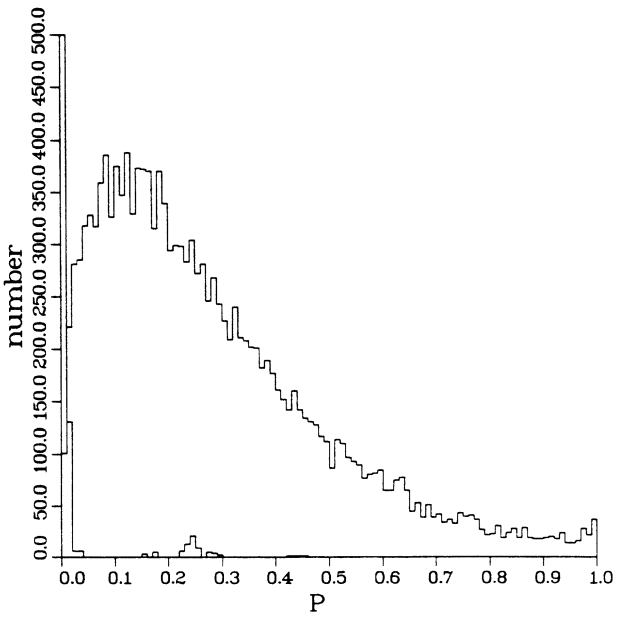

FIG. 11. Histogram of P for an equilibrium configuration of the small-E phase of the O(3) gauge theory at $\beta = 2.55$ (the broad distribution) and for the quenched configuration (sharply peaked at $P = 0$ and in the region $0.1 \leq P \leq 0.3$).

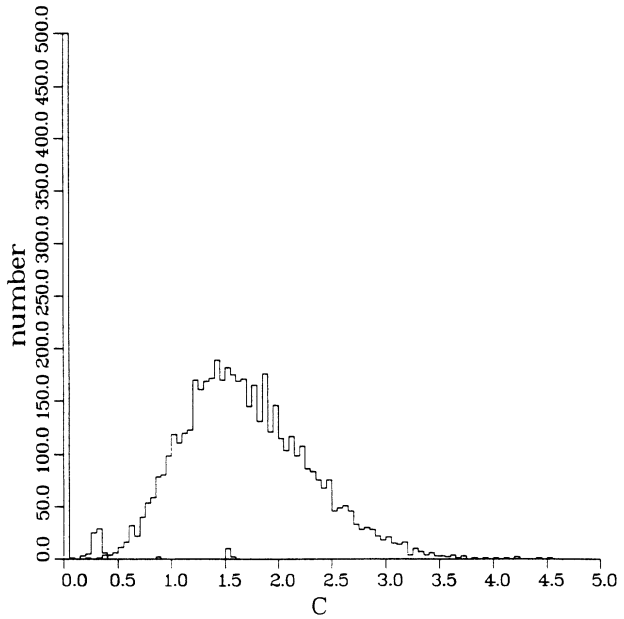

FIG. 12. Histogram of C for the same configurations as Fig. 11.

Figures 13–16 show similar histograms for the O(2) gauge field. Figures 13 and 14 are for an equilibrium configuration at $\beta = 1.0$ in the disordered phase, and its quenched configuration; $\bar{E}/P$ is 0.4469 for the starting configuration and 0.0377 for the quenched configuration. Figures 15 and 16 are for an equilibrium configuration at $\beta = 1.0$ in the correlated phase, and its quenched configuration; $\bar{E}/P$ is 0.3429 for the starting configuration and 0.0080 for the quenched configuration. The density of quenched monopoles is 0.029 for the large-E phase, and 0.006 for the small-E phase.

The striking similarity of the O(2) and O(3) results suggests that the mechanism of the phase transition is the same in the two models, associated with monopole formation as β decreases below β_c. This similarity is consistent with the results of a study of a model that interpolates between the O(3) and O(2) gauge theories.[11] The O(2) transition is weaker than the O(3) transition. Indeed there is some question whether the O(2) transition is of second order.[16] The weakness of the O(2) transition can be seen from Figs. 13 and 15. There is little difference between the P distributions of the small-E and large-E states. It follows that the latent heat of the transition is small. The difference between the states emerges after quenching: there are significantly more quenched monopoles from the large-E state. Again there is plenty of energy available in the small-E state to create monopoles, but the state is just not disordered in the right way to possess monopoles after quenching.

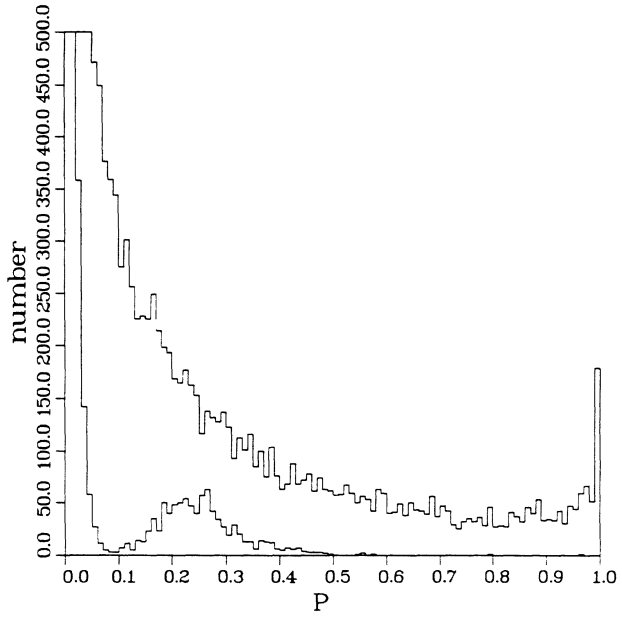

FIG. 13. Histogram of P for an equilibrium configuration of the large-E phase of the O(2) gauge theory at $\beta=1.0$ (the broad distribution) and for the quenched configuration (sharply peaked at $P=0$ and in the region $0.1 \leq P \leq 0.3$).

I have described relaxation calculations from equilibrium configurations at $\beta=\beta_c$. It is also interesting to consider states for other values of β in the hysteresis region. I find that the number of quenched monopoles is small (or large) for any small-E (or large-E) state in the hysteresis region. This is consistent with the fact that $F(E)$ has two local minima for β in the hysteresis region, corresponding to qualitatively different metastable phases.

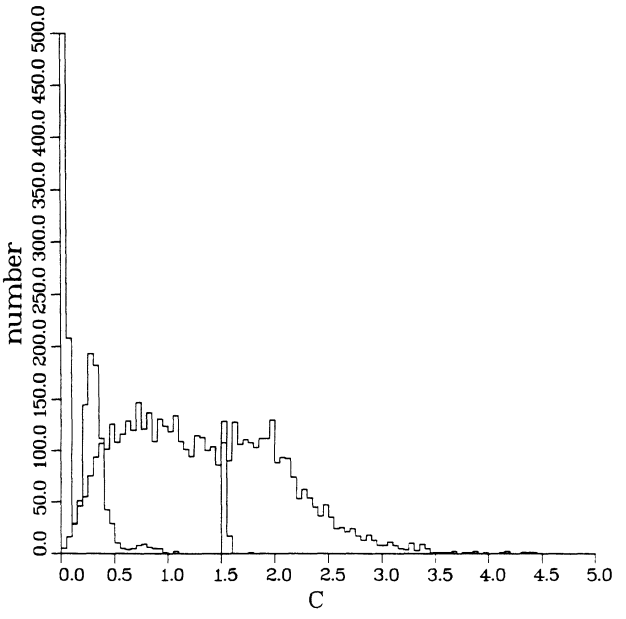

FIG. 14. Histogram of C for the same configurations as Fig. 13.

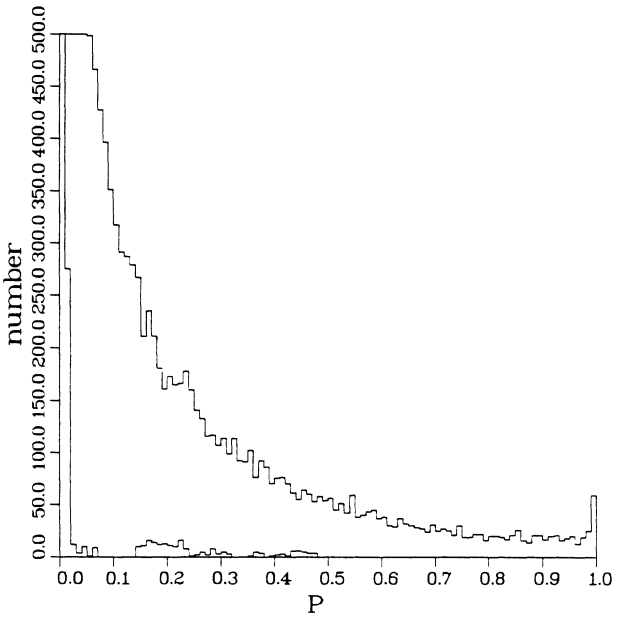

FIG. 15. Histogram of P for an equilibrium configuration of the small-E phase of the O(2) gauge theory at $\beta=1.0$ (the broad distribution) and for the quenched configuration (sharply peaked at $P=0$ and in the region $0.1 \leq P \leq 0.3$).

IV. DISCUSSION

The relaxation calculations of Sec. III demonstrate that the phase transitions of the O(3) and O(2) lattice gauge theories in four dimensions are associated with monopole topological configurations. In both cases, quenching the three-dimensional time slices of the configuration yields a significant density of monopoles in the large-E phase, but a negligible density in the small-E phase. Evidently the latent heat of the phase transition is

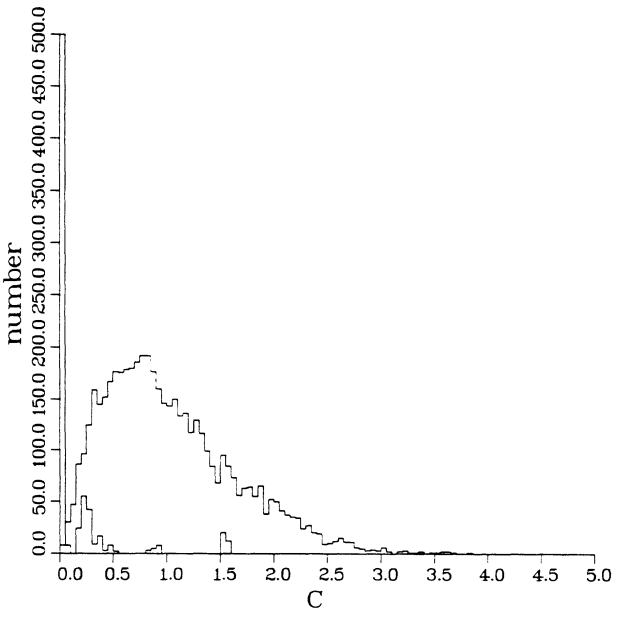

FIG. 16. Histogram of C for the same configurations as Fig. 15.

a combination of the energy needed to create the monopoles, plus the increase in energy of high-frequency fluctuations of the field in the presence of monopoles.

The O(3) and O(2) lattice gauge theories in *three* dimensions do *not* have phase transitions. Why is there no monopole-associated transition in three dimensions? The existence of the phase transition is determined by the form of the free energy $F(E)=E-S(E)/\beta$; a phase transition exists at β if $F(E)$ has a double minimum. This depends on the entropy $S(E)$ (Refs. 12 and 13). In the three-dimensional models, the entropy of ordered states, without monopoles, and that of disordered states, must join together smoothly in E, so there is no transition. In the four-dimensional models, there must be a kink in $S(E)$ at the value of E where monopoles begin to appear in three-dimensional subspaces, which causes the transition.

The O(3) gauge theory refers to the SU(2) gauge theory with adjoint action. What of the SU(2) gauge theory with fundamental action, i.e., the usual Wilson action? This model does not have a phase transition. The monopole-associated transition does not occur in this model because the monopole is not a stable, local minimum of the three-dimensional fundamental action. Obviously the O(3) monopole configuration, which has a Dirac string along which $U_4(p)\approx -1$, is not a low-energy configuration for the SU(2) action (6). Thus there is no action barrier to prevent the monopole from unwinding. Indeed, I find that quenching a random SU(2) configuration in three dimensions just produces the trivial zero field, or a gauge transformation of it. Therefore the free-energy function $F(E)$ has only a single local minimum for any β, because there is no well-defined separation in E of states with and without monopoles.

The quenching process considered in this paper is three dimensional. That is, time slices of the field configuration are relaxed, minimizing the three-dimensional energy. The three-dimensional quenching is interesting because the basic topological configuration of the O(3) or O(2) gauge theory is the monopole, a three-dimensional structure. But what is the result of full four-dimensional quenching? I find that for all of the models considered here, quenching the four-dimensional configuration, i.e., minimizing the four-dimensional action, does not produce well-separated monopoles in three dimensions. In particular, I do not observe monopoles propagating in the fourth dimension. Relaxing the links in all four dimensions apparently unwinds the three-dimensional topological singularities. Further research, perhaps requiring a more subtle analysis of the quenched configuration, may reveal the existence of other kinds of topological configurations in quenched four-dimensional fields, such as instantons.[15]

ACKNOWLEDGMENT

This work was supported by the National Science Foundation under Grant No. PHY-86-05967.

APPENDIX

To cast the O(2) gauge theory in the form of a U(1) gauge theory, write the O(2) link variable of Eq. (3) as

$$U_4(l)=\cos\theta(l),\quad U_3(l)=\sin\theta(l)\ . \tag{A1}$$

Then the plaquette variable for plaquette $p=(l_1,l_2,l_3,l_4)$ is

$$U_4(p)=\cos\theta(p),\quad U_3(p)=\sin\theta(p)\ , \tag{A2}$$

where

$$\theta(p)=\theta(l_1)+\theta(l_2)-\theta(l_3)-\theta(l_4)\ ; \tag{A3}$$

i.e., $\theta(p)$ is the lattice curl of $\theta(l)$. If Eq. (8) is used to define the action of the O(2) gauge theory, then the U(1) form is

$$E=\sum_p [1-\cos\theta(p)]\ ; \tag{A4}$$

if Eq. (9) is used, then the U(1) form is

$$E=\sum_p [1-\cos 2\theta(p)]\ . \tag{A5}$$

However, (A5) and (A4) are equivalent because a rescaling of $\theta(l)$, by $\theta(l)\rightarrow 2\theta(l)$, transforms (A4) into (A5).

[1]A. M. Polyakov, Nucl. Phys. **B120**, 429 (1977).
[2]T. Banks, R. Myerson, and J. Kogut, Nucl. Phys. **B129**, 493 (1977).
[3]D. R. Stump, Phys. Rev. D **23**, 972 (1981).
[4]T. DeGrand and D. Toussaint, Phys. Rev. D **22**, 2478 (1980).
[5]A. S. Kronfeld, G. Schierholz, and U.-J. Wiese, Nucl. Phys. **B293**, 461 (1987); J. Polonyi, *ibid.* **A461**, 279 (1987).
[6]K. Wilson, Phys. Rev. D **10**, 2445 (1974).
[7]I. G. Halliday and A. Schwimmer, Phys. Lett. **102B**, 337 (1981).
[8]G. Bhanot and M. Creutz, Phys. Rev. D **24**, 3212 (1981).
[9]G. Bhanot, Nucl. Phys. **B205**, 168 (1982).
[10]D. R. Stump, University of Edinburgh report (unpublished).
[11]D. R. Stump, Phys. Rev. D **38**, 1198 (1988).
[12]U. Heller and N. Seiberg, Phys. Rev. D **27**, 2980 (1983).
[13]J. H. Hetherington and D. R. Stump, Phys. Rev. D **35**, 1972 (1987); D. R. Stump and J. H. Hetherington, Phys. Lett. B **188**, 359 (1987).
[14]C. Kawabata and K. Binder, Solid State Commun. **22**, 705 (1977); S. Miyashita, H. Nishimori, A. Kuroda, and M. Suzuki, Prog. Theor. Phys. **60**, 1669 (1978).
[15]M. Teper, Phys. Lett. B **171**, 86 (1986).
[16]B. Lautrup and M. Nauenberg, Phys. Lett. **95B**, 63 (1980); K. J. M. Moriarty, Phys. Rev. D **25**, 2185 (1982); D. G. Caldi, Nucl. Phys. **B220**, 48 (1983); J. Jersak, T. Neuhaus, and P. M. Zerwas, Phys. Lett. **133B**, 103 (1983); H. G. Evertz, J. Jersak, T. Neuhaus, and P. M. Zerwas, Nucl. Phys. **B251**, 279 (1985).